

The effect of variable viscosity on the interfacial stability of two-layer Poiseuille flow

A. Pinarbasi and A. Liakopoulos^{a)}

Department of Mechanical Engineering and Mechanics, Lehigh University, Bethlehem, Pennsylvania 18015

(Received 18 November 1994; accepted 3 February 1995)

In this paper the linear stability analysis of the interface between two Newtonian liquids with temperature-dependent viscosity in plane Poiseuille flow is presented. A piecewise linear temperature profile is considered. The linearized equations describing the evolution of small, two-dimensional disturbances are derived and the stability problem is formulated as an eigenvalue problem for a set of ordinary differential equations. The continuous eigenvalue problem is solved numerically by a pseudospectral method based on Chebyshev polynomial expansions. The method leads to a generalized matrix eigenvalue problem, which is solved by the QZ algorithm. Results on the onset of instability are presented in the form of stability maps for a range of thickness ratios, disturbance wave numbers, imposed temperature differences, constant-temperature viscosity ratios, thermal conductivity ratios, and Reynolds numbers. Increasing the imposed temperature difference, constant-temperature viscosity ratio, or Reynolds number can have a stabilizing or destabilizing effect, depending on the flow configuration (thickness ratio) and disturbance wavelength. Increasing the thermal conductivity ratio has a destabilizing effect on the interface for all configurations and disturbance wavelengths. © 1995 American Institute of Physics.

I. INTRODUCTION

The hydrodynamic stability of viscous, two-fluid flow has become a subject of increasing interest in recent years due to its direct relation to the stability of operating states of several technologically important processes. In the petroleum industry, for example, when water is added to the high-viscosity crude oil flowing through pipelines, the less viscous water encapsulates the oil and coats the inner pipe walls, thus reducing the pumping costs considerably (Yu and Sparrow,¹ Hu and Joseph²). In coextrusion operations, multilayer sheets and films take their final form, as they flow side by side through appropriately designed dies. The process is limited by the onset of interfacial instabilities at high extrusion rates or high values of the viscous stratification parameter, thus deteriorating the mechanical, optical, and barrier properties of the final product (Han,³ Pinarbasi and Liakopoulos⁴).

Several researchers have investigated the onset of interfacial instabilities, due to viscosity stratification for isothermal flow of Newtonian fluids (Yih,⁵ Yiantsios and Higgins,⁶ Hooper,⁷ and Anturkar *et al.*⁸). To the best of the authors' knowledge, no study on interfacial instability in nonisothermal, two-fluid channel flow has been reported, although in many applications (especially in the coextrusion processes) temperature variations cannot be ignored. For single-fluid plane Poiseuille flow, temperature-dependent viscosity has a strong effect on the *shear* mode of instability. Potter and Graber⁹ found that there is a 50% reduction in critical Reynolds number for a 78 K wall temperature difference in water flow. Recently, Schäfer and Herwig¹⁰ reexamined the stability of single-fluid Poiseuille flow and investigated the effect of temperature variations using asymptotics and a Taylor series expansion of viscosity with respect to temperature.

In this paper, we address the question of variable viscos-

ity effects on the *interfacial* instability mode in two-layer channel flow driven by a pressure gradient. We assume that the dominant variable property effect is the dependence of viscosity on temperature. Base flow equations, perturbation evolution equations, and interfacial boundary conditions are derived by taking into account the variation of viscosity with temperature. A piecewise linear temperature profile is considered. The stability problem is formulated as an eigenvalue problem for a set of ordinary differential equations. Discretization is performed using a pseudospectral method based on Chebyshev polynomial expansions. The resulting generalized matrix eigenvalue problem is solved using the QZ algorithm.

II. GOVERNING EQUATIONS

We consider nonisothermal flow of two immiscible, incompressible, Newtonian fluids in a straight channel (Fig. 1). The flow is driven by a constant pressure gradient acting along the channel axis. Fluid viscosities depend on the local temperature. The continuity and momentum balance equations for the *k*th layer can be written as

$$\frac{\partial \bar{u}_i^k}{\partial \bar{x}_i} = 0, \quad (1)$$

$$\bar{\rho}_k \left(\frac{\partial \bar{u}_j^k}{\partial \bar{t}} + \bar{u}_i^k \frac{\partial \bar{u}_j^k}{\partial \bar{x}_i} \right) = - \frac{\partial \bar{p}^k}{\partial \bar{x}_j} + \frac{\partial \bar{\tau}_{ij}^k}{\partial \bar{x}_i}, \quad j=1,2 \quad (\text{no summation over } k), \quad (2)$$

where the summation convention is used over index *i*. In the equations above, $\bar{\rho}$ denotes the fluid density, \bar{p} is the pressure, \bar{u}_i is the *i*th component of the velocity vector, $\bar{\tau}_{ij}$ is the (*i,j*)th component of the deviatoric stress tensor, and *k* denotes the layer number. For Newtonian, incompressible liquids,

^{a)}Telephone: (610) 758 4929; Electronic-mail: al03@lehigh.edu

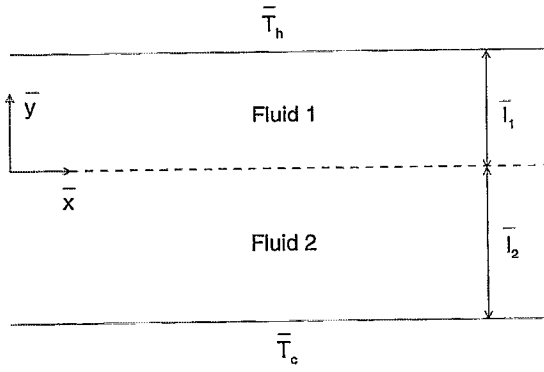


FIG. 1. Flow domain.

$$\bar{\tau}_{ij}^k = \bar{\mu}_k \left(\frac{\partial \bar{u}_i^k}{\partial \bar{x}_j} + \frac{\partial \bar{u}_j^k}{\partial \bar{x}_i} \right) \quad (\text{no summation over } k),$$

and the empirical viscosity–temperature relationship is of the form

$$\bar{\mu}_k = c_k \bar{\mu}_{0k} \exp(\bar{d}_k / \bar{T}_k). \quad (3)$$

In Eq. (3), $\bar{\mu}_{0k}$ is the viscosity calculated at the reference temperature, c_k and \bar{d}_k are constants determined from viscosity–temperature empirical curves, and \bar{T}_k is the local temperature, all for the k th layer.

Introducing dimensionless variables based on the interfacial velocity, \bar{U}_0 , and the thickness of the upper layer, \bar{l}_1 , i.e.,

$$u_i = \frac{\bar{u}_i}{\bar{U}_0}, \quad x_i = \frac{\bar{x}_i}{\bar{l}_1}, \quad m_k = \frac{\bar{\mu}_{0k}}{\bar{\mu}_{01}}, \quad r_k = \frac{\bar{\rho}_k}{\bar{\rho}_1},$$

$$t = \frac{\bar{t} \bar{U}_0}{\bar{l}_1}, \quad p = \frac{\bar{p}}{\bar{\rho}_1 \bar{U}_0^2}, \quad \mu_k = \frac{\bar{\mu}_k}{\bar{\mu}_{01}},$$

the governing equations become

$$\frac{\partial u_i^k}{\partial x_i} = 0, \quad (4)$$

$$\frac{\partial u_j^k}{\partial t} + u_i^k \frac{\partial u_j^k}{\partial x_i} = -\frac{1}{r_k} \frac{\partial p^k}{\partial x_j} + \frac{1}{\text{Re } r_k} \frac{\partial \tau_{ij}^k}{\partial x_i}, \quad j=1,2. \quad (5)$$

In Eq. (5),

$$\tau_{ij}^k = \mu_k \left(\frac{\partial u_i^k}{\partial x_j} + \frac{\partial u_j^k}{\partial x_i} \right),$$

$$\mu_k = c_k m_k \exp(\bar{d}_k / \bar{T}_k), \quad (6)$$

where $m_k = \bar{\mu}_{0k} / \bar{\mu}_{01}$ is the constant-temperature viscosity ratio and $r_k = \bar{\rho}_k / \bar{\rho}_1$ is the density ratio, both for the k th layer. Here, the Reynolds number is defined as $\text{Re} = \bar{\rho}_1 \bar{U}_0 \bar{l}_1 / \bar{\mu}_{01}$.

A. Base temperature and flow fields

The undisturbed base flow is assumed to be fully developed. Considering a temperature field that is independent of

x , the energy balance equation (neglecting viscous dissipation and variable thermal conductivity effects) yields a linear temperature profile in each layer. This solution of the energy equation is realizable only for isothermal channel walls. Denoting the upper hot wall temperature by \bar{T}_h and the lower cold wall temperature by \bar{T}_c , the temperature distribution becomes

$$\frac{\bar{T}_k(y) - \bar{T}_c}{\Delta \bar{T}} = A_k y + \epsilon A_2, \quad k=1,2, \quad (7)$$

where $\Delta \bar{T} = \bar{T}_h - \bar{T}_c$ is the wall temperature difference, $\epsilon = \bar{l}_2 / \bar{l}_1$ is the fluid-layer thickness ratio, $A_1 = K_2 / (K_2 + \epsilon)$, $A_2 = A_1 / K_2$, and $K_2 = \bar{k}_2 / \bar{k}_1$ is the thermal conductivity ratio. Substituting Eq. (7) into Eq. (6) gives

$$\mu_k = c_k m_k \exp\left(\frac{1}{S_k y + Q_k}\right), \quad k=1,2, \quad (8)$$

where $S_k = a_k A_k$, $Q_k = \epsilon a_k A_2 + b_k$, $a_k = \Delta \bar{T} / \bar{d}_k$, and $b_k = \bar{T}_c / \bar{d}_k$. The temperature of the cold wall is chosen as the reference temperature in viscosity calculations.

Switching from indicial notation i, j to conventional x, y notation, the x component of the momentum equation takes the form

$$\left[\exp\left(\frac{1}{S_k y + Q_k}\right) u_{b_k}' \right]' = E_k, \quad k=1,2, \quad (9)$$

where $E_k = \text{Re}(dp/dx) / (c_k m_k)$, dp/dx is the dimensionless pressure gradient, u_{b_k} denotes the base velocity of the k th layer, and primes denote differentiation with respect to y .

The associated boundary conditions (no slip at the channel walls and continuity of velocity and shear stress at the interface) are expressed in dimensionless form by

$$u_{b_1}(1) = u_{b_2}(-\epsilon) = 0, \quad (10a)$$

$$u_{b_1}(0) = u_{b_2}(0), \quad (10b)$$

$$\mu_1(0) u_{b_1}'(0) = \mu_2(0) u_{b_2}'(0). \quad (10c)$$

The solution of differential equation (9) that satisfies boundary conditions (10a)–(10c) is found to be

$$u_{b_1}(y) = \frac{E_1}{2S_1^2} \left\{ (S_1 y + Q_1)(B_1 - Q_1 - 1 + S_1 y) \right. \\ \times \exp\left(-\frac{1}{S_1 y + Q_1}\right) - (S_1 + Q_1)(B_1 - Q_1 - 1 + S_1) \\ \times \exp\left(-\frac{1}{S_1 + Q_1}\right) + (B_1 - 2Q_1 - 1) \\ \left. \times \left[E\left(\frac{1}{S_1 + Q_1}\right) - E\left(\frac{1}{S_1 y + Q_1}\right) \right] \right\}, \quad (11)$$

$$\begin{aligned}
u_{b_2}(y) = & \frac{E_2}{2S_2^2} \left\{ (S_2y + Q_2)(B_3 - Q_2 - 1 + S_2y) \right. \\
& \times \exp\left(-\frac{1}{S_2y + Q_2}\right) - (Q_2 - \epsilon S_2) \\
& \times (B_3 - Q_2 - 1 - \epsilon S_2) \exp\left(-\frac{1}{Q_2 - \epsilon S_2}\right) \\
& \left. + (B_3 - 2Q_2 - 1) \left[E\left(\frac{1}{Q_2 - \epsilon S_2}\right) - E\left(\frac{1}{S_2y + Q_2}\right) \right] \right\}, \quad (12)
\end{aligned}$$

where $E(x) = \int_x^\infty (e^{-t}/t) dt$ is the exponential integral (Abramowitz and Stegun¹¹),

$$B_1 = \frac{(c_2/c_1)m_2f_3 + (S_1/S_2)f_4}{(c_2/c_1)m_2f_2 - f_1},$$

$$B_3 = \frac{S_2}{S_1} B_1,$$

and

$$\begin{aligned}
f_1 = & \frac{Q_2}{S_2} e^{-1/Q_2} - \frac{Q_2 - \epsilon S_2}{S_2} e^{-1/(Q_2 - \epsilon S_2)} \\
& + \frac{1}{S_2} \left[E\left(\frac{1}{Q_2 - \epsilon S_2}\right) - E\left(\frac{1}{Q_2}\right) \right],
\end{aligned}$$

$$\begin{aligned}
f_2 = & \frac{Q_1}{S_1} e^{-1/Q_1} - \frac{Q_1 + S_1}{S_1} e^{-1/(Q_1 + S_1)} \\
& + \frac{1}{S_1} \left[E\left(\frac{1}{Q_1 + S_1}\right) - E\left(\frac{1}{Q_1}\right) \right],
\end{aligned}$$

$$\begin{aligned}
f_3 = & \frac{Q_1 + Q_2^2}{S_1} e^{-1/Q_1} \\
& + \frac{(Q_1 + S_1)(S_1 - Q_1 - 1)}{S_1} e^{-1/(Q_1 + S_1)} \\
& + \frac{2Q_1 + 1}{S_1} \left[E\left(\frac{1}{Q_1 + S_1}\right) - E\left(\frac{1}{Q_1}\right) \right],
\end{aligned}$$

$$\begin{aligned}
f_4 = & -\frac{Q_2 + Q_2^2}{S_2} e^{-1/Q_2} \\
& + \frac{(Q_2 - \epsilon S_2)(\epsilon S_2 + Q_2 + 1)}{S_2} e^{-1/(Q_2 - \epsilon S_2)} \\
& - \frac{2Q_2 + 1}{S_2} \left[E\left(\frac{1}{Q_2 - \epsilon S_2}\right) - E\left(\frac{1}{Q_2}\right) \right].
\end{aligned}$$

The pressure gradient dp/dx is found by using the condition $u_{b_1}(0) = 1$. The constants c_k and \bar{d}_k depend on the fluid and reference temperature chosen.

B. Linear stability analysis

In this section, we formulate the stability problem by the method of small disturbances. Temperature fluctuations are neglected (Wazzan *et al.*¹²). Their effect on instability has

been shown to be small in single-layer Poiseuille flow (Schäfer and Herwig¹⁰) and in flat-plate boundary-layer flow (Herwig and Schäfer¹³). The velocity and pressure fields are disturbed by imposing two-dimensional, infinitesimal disturbances on the base flow, i.e.,

$$u_k(x, y, t) = u_{b_k}(y) + \hat{u}_k(x, y, t),$$

$$v_k(x, y, t) = \hat{v}_k(x, y, t), \quad (13)$$

$$p_k(x, y, t) = p_{b_k}(x) + \hat{p}_k(x, y, t).$$

Substitution of Eq. (13) into Eqs. (4) and (5), subtraction of the base flow equations, and linearization lead to the disturbance evolution equations,

$$\frac{\partial \hat{u}^k}{\partial x} + \frac{\partial \hat{v}^k}{\partial y} = 0, \quad (14)$$

$$\begin{aligned}
\frac{\partial \hat{u}^k}{\partial t} + u_b^k \frac{\partial \hat{u}^k}{\partial x} + \hat{v}^k \frac{du_b^k}{dy} \\
= -\frac{1}{r_k} \frac{\partial \hat{p}^k}{\partial x} + \frac{\mu_k}{\text{Re } r_k} \left(\frac{\partial^2 \hat{u}^k}{\partial x^2} + \frac{\partial^2 \hat{u}^k}{\partial y^2} \right) \\
+ \frac{\mu_k'}{\text{Re } r_k} \left(\frac{\partial \hat{u}^k}{\partial y} + \frac{\partial \hat{v}^k}{\partial x} \right), \quad (15a)
\end{aligned}$$

$$\begin{aligned}
\frac{\partial \hat{v}^k}{\partial t} + u_b^k \frac{\partial \hat{v}^k}{\partial x} = -\frac{1}{r_k} \frac{\partial \hat{p}^k}{\partial y} + \frac{\mu_k}{\text{Re } r_k} \left(\frac{\partial^2 \hat{v}^k}{\partial y^2} + \frac{\partial^2 \hat{v}^k}{\partial x^2} \right) \\
+ \frac{2\mu_k'}{\text{Re } r_k} \frac{\partial \hat{v}^k}{\partial y}, \quad (15b)
\end{aligned}$$

where primes denote differentiation with respect to y and $k=1,2$.

The continuity equation for the disturbances, Eq. (14), is satisfied by introducing a perturbation streamfunction, $\hat{\psi}_k$, for each layer, i.e.,

$$\hat{u}_k = \frac{\partial \hat{\psi}_k}{\partial y}, \quad \hat{v}_k = -\frac{\partial \hat{\psi}_k}{\partial x}, \quad k=1,2.$$

It is further assumed that all disturbances have time and spatial dependence of the form (Drazin and Reid,¹⁴ Simpkins and Liakopoulos¹⁵),

$$(\hat{\psi}_k, \hat{p}_k) = [\phi_k(y), f_k(y)] e^{i\alpha(x-ct)}, \quad k=1,2, \quad (16)$$

where α is the wave number, c is the complex velocity, and ϕ_k, f_k denote the spatially varying disturbance amplitudes.

Substituting Eq. (16) into the linearized momentum equations, Eqs. (15), and eliminating the pressure perturbation terms by cross-differentiation, the stability governing equations become

$$\begin{aligned}
i\alpha \text{Re } r_k [(u_{b_k} - c)(\phi_k'' - \alpha^2 \phi_k) - u_{b_k}'' \phi_k] \\
= \mu_k (\phi_k^{\text{IV}} - 2\alpha^2 \phi_k'' + \alpha^4 \phi_k) + 2\mu_k' (\phi_k''' - \alpha^2 \phi_k') \\
+ \mu_k'' (\phi_k'' + \alpha^2 \phi_k), \quad k=1,2. \quad (17)
\end{aligned}$$

These equations differ from the usual Orr–Sommerfeld equations, in that they contain viscosity derivative terms.

The associated boundary conditions are the following:

- no slip at solid walls,

$$\phi_1 = \phi_1' = 0, \quad \text{at } y=1,$$

$$\phi_2 = \phi_2' = 0, \quad \text{at } y = -\epsilon; \quad (18a)$$

- continuity of velocities at the fluid–fluid interface (applied at $y=0$),

$$\phi_1 = \phi_2, \quad \phi_1' - \phi_2' = \frac{\phi_1}{c - u_{b1}} (u_{b2}' - u_{b1}'); \quad (18b)$$

- continuity of shear stress at the fluid–fluid interface (applied at $y=0$),

$$\mu_1(\alpha^2 \phi_1 + \phi_1'') = \mu_2(\alpha^2 \phi_2 + \phi_2''); \quad (18c)$$

- and continuity of normal stress at the fluid–fluid interface (applied at $y=0$),

$$\begin{aligned} & \mu_2 \phi_2''' + \mu_2' \phi_2'' - (3\mu_2 \alpha^2 + i\alpha \text{Re } r_2 u_{b2}') \phi_2' \\ & + (\mu_2' \alpha^2 + i\alpha \text{Re } r_2 u_{b2}') \phi_2 - \mu_1 \phi_1''' - \mu_1' \phi_1'' \\ & + (3\mu_1 \alpha^2 + i\alpha \text{Re } u_{b1}') \phi_1' - (\mu_1' \alpha^2 \\ & + i\alpha \text{Re } u_{b1}') \phi_1 - c(i\alpha \text{Re } \phi_1' - i\alpha \text{Re } r_2 \phi_2') \\ & = i\alpha \text{Re}(F + \alpha^2 S) \frac{\phi_1}{c - u_{b1}}; \end{aligned} \quad (18d)$$

where $S = \bar{\sigma}/\rho_1 \bar{U}_0^2 \bar{l}_1$ and $F = (\bar{\rho}_2 - \bar{\rho}_1) \bar{g} \bar{l}_1 / (\rho_1 \bar{U}_0^2)$ are dimensionless groups accounting for the effects of interfacial tension, $\bar{\sigma}$, and gravitational acceleration, \bar{g} .

In this paper, we approach the stability question as a temporal stability problem, i.e., for an arbitrary positive real value of α , we seek solutions to the resulting eigenanalysis problem and obtain the complex eigenvalue c and the corresponding eigenfunction ϕ_k . The sign of c_i determines the stability of the flow, i.e., if $c_i > 0$ the flow is temporally unstable.

C. Method of solution

The continuous eigenvalue problem formulated in the previous section is discretized using a pseudospectral tech-

TABLE I. Comparison of asymptotic and numerical results for $\Delta \bar{T} \rightarrow 0$. Here $\text{Re}=10$, $r_2=1$, $F=S=0$, $\epsilon=1$, and $\alpha=1 \times 10^{-2}$.

m_2	c	
	Asymptotic (Yih, ⁵)	Numerical (present study, $N=12$) $\Delta \bar{T}=0.01$
10	$1.67219 + i1.24810 \times 10^{-3}$	$1.67240 + i1.24858 \times 10^{-3}$
20	$2.06020 + i1.58950 \times 10^{-3}$	$2.06029 + i1.59039 \times 10^{-3}$
100	$2.71932 + i2.05299 \times 10^{-2}$	$2.71924 + i2.05586 \times 10^{-2}$

nique. Each layer in the physical space, $0 \leq y \leq 1$, and $-\epsilon \leq y \leq 0$, is transformed to $-1 \leq Y \leq 1$. The functions ϕ_k , $k=1,2$, are expanded in series of Chebyshev polynomials. Truncating each series after N terms, $N+1$ expansion coefficients are introduced as unknowns in each layer. In each layer, the method of point collocation is applied to Eqs. (17) at

$$Y_j = \cos\left(\frac{\pi j}{N-4}\right), \quad j=0,1,2,\dots,N-4.$$

The resulting $(2N-6)$ equations are supplemented by the discrete versions of the eight boundary conditions, Eqs. (18a)–(18d), to obtain $2(N+1)$ equations. This procedure results in a generalized matrix eigenvalue problem of the form $Ax = cBx$, which is solved using *dgvlgc*, an IMSL routine that implements the QZ algorithm. The calculations were performed in double-precision arithmetic on an IBM 6000 workstation. Up to $N=20$ terms were used in each layer to achieve convergence in the computation of eigenvalues.

The computer implementation of the numerical procedure outlined above was tested by comparison with Yih's⁵ asymptotic results for isothermal, two-layer flow. As $\Delta \bar{T} \rightarrow 0$ our numerical results are in very good agreement with Yih's⁵ data (Table I).

III. RESULTS AND DISCUSSION

The dependence of viscosity of Newtonian liquids on temperature is adequately modeled by Eq. (3). For a standard transformer oil–water system (water at the bottom layer),

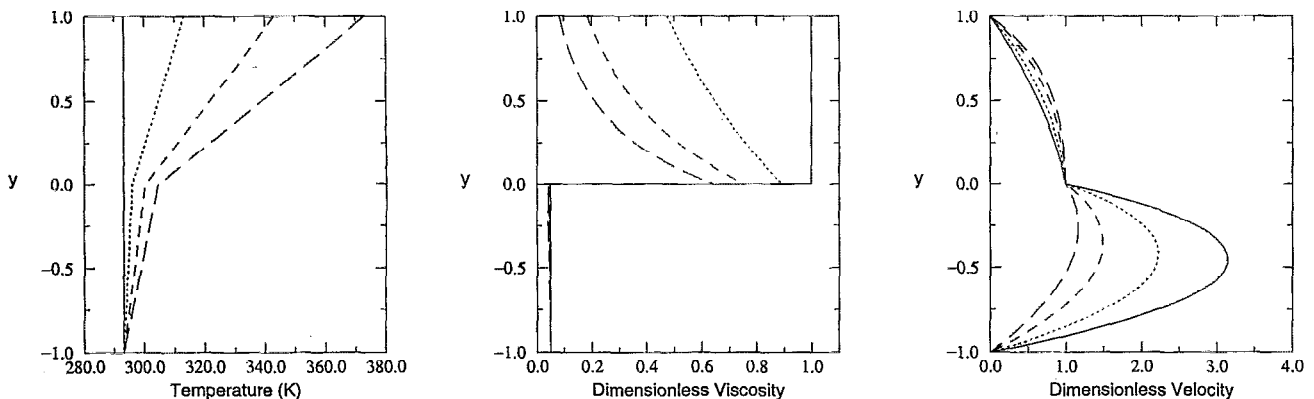


FIG. 2. Temperature, viscosity, and velocity profiles. Here $\text{Re}=0.1$, $r_2=1$, $F=S=0$, $m_2=0.05$, $K_2=6$, and $\epsilon=1$. Viscosity-law constants are as in the text. —: $\Delta T=0$ K; \cdots : $\Delta T=20$ K; $---$: $\Delta T=50$ K; and $- \cdot -$: $\Delta T=80$ K.

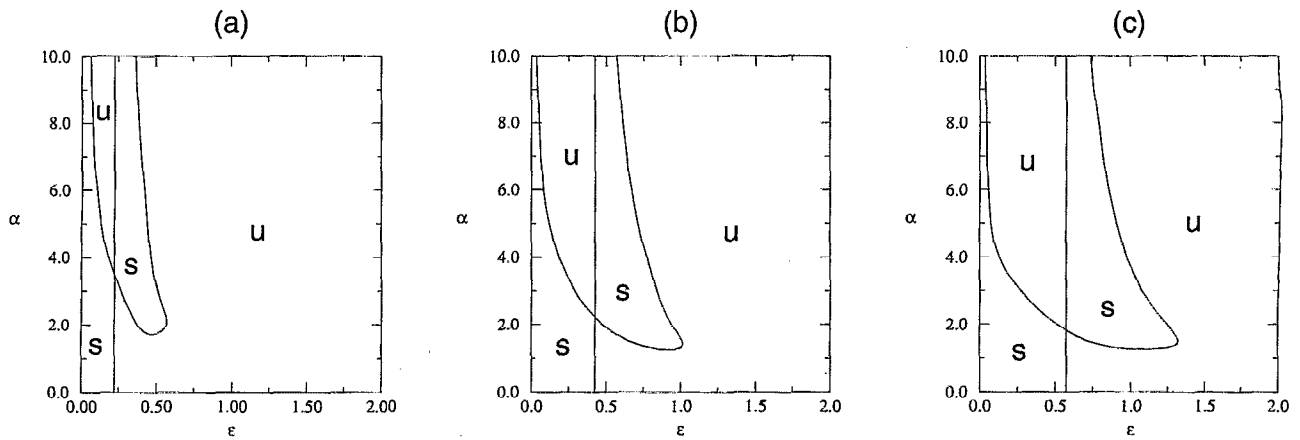


FIG. 3. Effect of wall temperature difference ΔT on interfacial stability. Here $Re=0.1$, $r_2=1$, $F=S=0$, $m_2=0.05$, and $K_2=6$. Viscosity-law constants are as in the text. (a) $\Delta T=0$ K, (b) $\Delta T=50$ K, and (c) $\Delta T=80$ K.

choosing the reference temperature to be 20°C gives $c_1=8.836\times 10^{-6}$, $c_2=2.125\times 10^{-3}$, $\bar{d}_1=3411.3$ K, and $\bar{d}_2=1804.1$ K. For the same fluid system, $K_2=6$ and $m_2=0.05$. Figure 2 shows the temperature, viscosity, and velocity profiles for $Re=0.1$, $r_2=1$, $m_2=0.05$, $\epsilon=1$, $K_2=6$, and $\Delta\bar{T}=\bar{T}_h-\bar{T}_c=0, 20, 50$, and 80 K. Since the viscosity of liquids decreases with increasing temperature, the resultant dimensionless velocity profiles become skewed as $\Delta\bar{T}$ increases and its maximum shifts toward the hotter wall. Furthermore, it is pointed out that the Reynolds number is defined here, based on the velocity at the interface. Consequently, if all the reference parameters are fixed, e.g., in a particular experimental setting, a change in the temperature difference across the channel, $\Delta\bar{T}$, leads to a corresponding change in the value of the Reynolds number.

The effect of wall temperature difference $\Delta\bar{T}$ on the interface stability is shown in Fig. 3 in the (ϵ, α) plane. The values of the parameters $Re=0.1$, $r_2=1$, $F=S=0$, $m_2=0.05$, and $K_2=6$ are kept fixed, while $\Delta\bar{T}$ takes the values 0, 50, and 80 K. In all cases, there exists a straight line, $\epsilon=\text{const}$, along which the flow is neutrally stable for all wave num-

bers. The value of ϵ along this line corresponds to the thickness ratio, for which the slope of the base flow velocity profile is continuous across the fluid–fluid interface, and it will be referred to as the critical thickness ratio, ϵ_{cr} . For isothermal flow, $\epsilon_{cr} = \sqrt{m_2}$. Increasing the wall temperature difference $\Delta\bar{T}$ results in shifting ϵ_{cr} to the right [see Figs. 3(b) and 3(c)]. In addition, increasing $\Delta\bar{T}$ destabilizes the region to the left of ϵ_{cr} , while it has stabilizing effect on the region to the right of ϵ_{cr} .

For $\epsilon \ll 1$ and $\epsilon \gg 1$, our results show that the thin layer effect observed for isothermal flows (Hooper,¹⁶ Renardy,¹⁷ and Joseph *et al.*¹⁸) persists, even in highly nonisothermal flows in the range of parameters studied. Flows with a very thin layer of the less viscous fluid next to the wall are stable. In contrast, a thin layer of more viscous fluid adjacent to the solid boundary is linearly unstable to an interfacial instability mode. As shown in Fig. 3(a) (isothermal flow conditions), when the thickness of the less viscous fluid is very small, i.e., $\epsilon \ll 1$, there exists a stable region for all wave numbers. This window of stability exists also for nonisothermal flows.

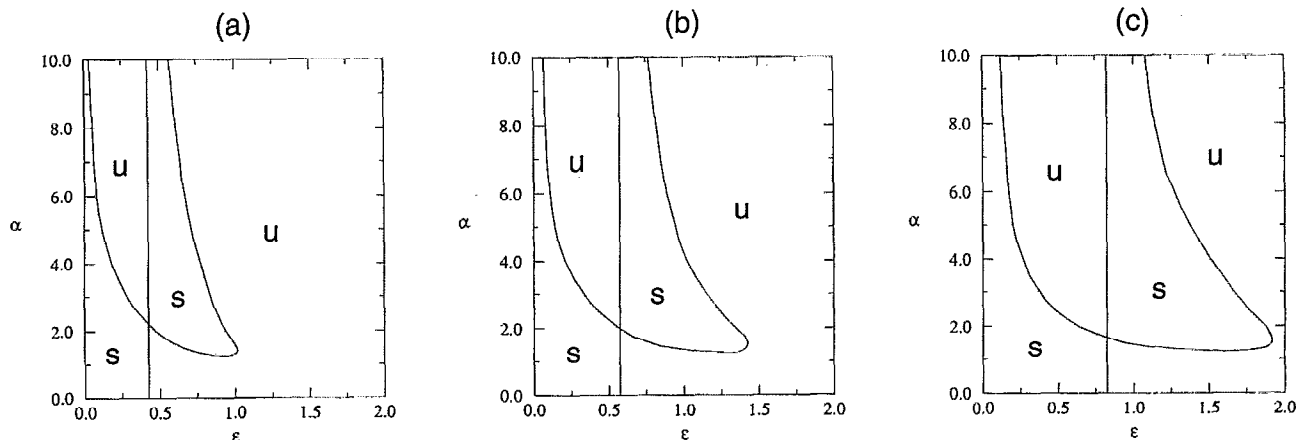


FIG. 4. Effect of constant-viscosity ratio m_2 on interfacial stability. Here $Re=0.1$, $r_2=1$, $F=S=0$, $K_2=6$, and $\Delta T=50$ K. (a) $m_2=0.05$, (b) $m_2=0.1$, and (c) $m_2=0.2$.

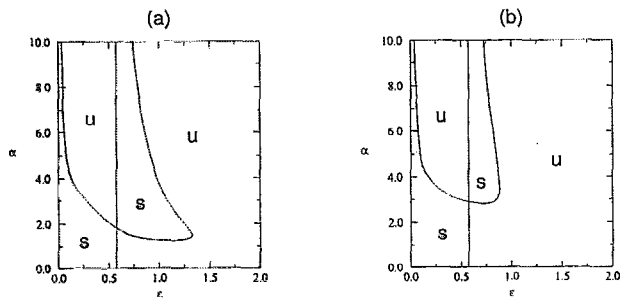


FIG. 5. Effect of the Reynolds number on interfacial stability. Here $F=S=0$, $m_2=0.05$, $K_2=6$, $r_2=1$, and $\Delta T=80$ K. (a) $Re=0.1$, (b) $Re=10$.

However, as ΔT increases, the thickness of the less viscous fluid should be reduced even more in order to obtain a stable interface. Although our results are reported for the interval $0 \leq \epsilon \leq 2$, we have extended our stability calculations up to $\epsilon=10$. For $2 \leq \epsilon \leq 10$, the flow is unstable for all wave numbers, in agreement with the thin layer effect reported for isothermal flows.

For single-fluid, plane, Poiseuille flow, Potter and Graber⁹ showed that temperature-dependent viscosity has a strong effect on shear instability and a nonzero wall temperature difference is always destabilizing. Our study focuses on interfacial instabilities of two-layer flows, which can be triggered at low values of Reynolds number. Temperature-dependent viscosity has a strong effect on interfacial instability, but an imposed wall temperature difference can stabilize or destabilize the interface depending on the flow configuration and disturbance wavelength.

Figure 4 shows the effect of constant-temperature viscosity ratio m_2 on interfacial stability. The values $Re=0.1$, $r_2=1$, $F=S=0$, $K_2=6$, and $\Delta T=50$ K are kept fixed, while m_2 is set to 0.05, 0.1, and 0.2 in Figs. 4(a)–4(c), respectively. It is seen that the effect of m_2 on interfacial stability is qualitatively similar to that of ΔT . However, the shift in ϵ_{cr} , the enlargement of the unstable region to the left of ϵ_{cr} and of the stable region to the right of ϵ_{cr} are considerably more pronounced as m_2 increases. As was pointed out by one of the reviewers, the fact that the influence of m_2 on the flow stability is qualitatively similar to that of ΔT may be explained as follows. A larger wall temperature difference, ΔT , increases the effective viscosity ratio of the two liquids, since the viscosity of the layer next to the hot plate is reduced to a larger extent than the viscosity of the layer next to the cold plate (see Fig. 2).

The effect of Reynolds number, Re , on the interfacial instability is presented in Fig. 5. Here, $r_2=1$, $F=S=0$, $K_2=6$, $m_2=0.05$, and $\Delta T=80$ K are kept fixed while $Re=0.1$ in Fig. 5(a) and $Re=10$ in Fig. 5(b). Increasing Re has clearly a destabilizing effect for $\epsilon > \epsilon_{cr}$. A slight stabilizing effect is noticed in the region to the left of ϵ_{cr} . In some sense, for fixed ΔT , the effect of Re on the interfacial stability is opposite of the effect of m_2 . However, the most pronounced feature of the maps presented in Fig. 5 is the reduction of the size of the stable region for $\epsilon > \epsilon_{cr}$. For $\epsilon > \epsilon_{cr}$, the stable region in the neutral stability map is shifted toward larger

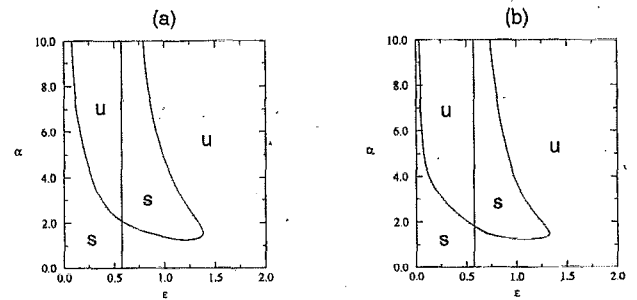


FIG. 6. Effect of thermal conductivity ratio K_2 on interfacial stability. Here $Re=0.1$, $r_2=1$, $F=S=0$, $m_2=0.05$, and $\Delta T=80$ K. (a) $K_2=0.05$, (b) $K_2=6$.

values of α . This effect is more pronounced for the nonisothermal flow conditions examined in the present paper than for isothermal conditions (compare with Fig. 5 of Ref. 6).

In Fig. 6, we present the effect of thermal conductivity ratio K_2 on the interfacial stability. Here, $Re=0.1$, $r_2=1$, $F=S=0$, $m_2=0.05$, and $\Delta T=80$ K, while the value of K_2 is 0.05 in Fig. 6(a) and 6 in Fig. 6(b). The unstable region to the left of ϵ_{cr} is enlarged, while the stable region to the right of ϵ_{cr} diminishes as K_2 increases. Therefore, the overall effect of increasing K_2 is destabilizing.

A quantitative analysis of the influence of nonzero surface tension ($S \neq 0$) on interface stability is beyond the scope of the present paper. On physical grounds, it is expected that the influence of S on the stability maps presented in Figs. 3–6 will be negligible for $\alpha \rightarrow 0$. In contrast, the presence of interfacial tension will stabilize the interface for intermediate and short wave disturbances (large values of α) at all layer thickness ratios, ϵ . This behavior is also predicted by the stability analysis of the isothermal system.⁶

IV. CONCLUSIONS

A two-dimensional, linear stability analysis of two-layer, plane, Poiseuille flow of Newtonian liquids with temperature-dependent viscosity has been presented. The temperature profile is linear within each layer, temperature perturbations are neglected, and an exponential viscosity law is assumed. In the absence of density stratification and interfacial tension effects, it is found that increasing the wall temperature difference ΔT or the constant-temperature viscosity ratio m_2 destabilizes the region to the left of ϵ_{cr} (ϵ_{cr} is the critical thickness ratio) and stabilizes the region to the right of ϵ_{cr} in the (ϵ, α) plane. For fixed ΔT , the effect of Re on the interfacial stability is opposite of the effect of m_2 . Therefore, increasing ΔT , m_2 , or Re can have a stabilizing or destabilizing effect, depending on the flow configuration and disturbance wavelength. Increasing thermal conductivity ratio K_2 destabilizes the interface. The thin layer effect observed in isothermal flows persists in the nonisothermal flows investigated in the present study.

ACKNOWLEDGMENTS

This work was partially supported by National Science Foundation under Grant No. DDM-9110850 and by NASA/LeRC under Contract No. NAG3-1632.

- ¹H. S. Yu and E. M. Sparrow, "Experiments on two-component stratified flow in a horizontal duct," *J. Heat Transfer C* **91**, 51 (1969).
- ²H. H. Hu and D. D. Joseph, "Lubricated pipelining: Stability of core-annular flow. Part 2," *J. Fluid Mech.* **205**, 359 (1989).
- ³C. D. Han, *Multiphase Flow in Polymer Processing* (Academic, New York, 1981).
- ⁴A. Pinarbasi, and A. Liakopoulos, "Stability of two-layer Poiseuille flow of Carreau-Yasuda and Bingham-like fluids," *J. Non-Newtonian Fluid Mech.* (in press).
- ⁵C. S. Yih, "Instability due to viscosity stratification," *J. Fluid Mech.* **27**, 337 (1967).
- ⁶S. G. Yiantsios and B. G. Higgins, "Linear stability of plane Poiseuille flow of two superposed fluids," *Phys. Fluids* **31**, 3225 (1988).
- ⁷A. P. Hooper, "The stability of two superposed fluids in a channel," *Phys. Fluids* **1**, 1133 (1989).
- ⁸N. R. Anturkar, T. C. Papanastasiou, and J. O. Wilkes, "Linear stability analysis of multilayer plane Poiseuille flow," *Phys. Fluids* **2**, 530 (1990).
- ⁹M. C. Potter and E. J. Graber, "Stability of plane Poiseuille flow with heat transfer," NASA TN D-6027, 1970.
- ¹⁰P. Schäfer and H. Herwig, "Stability of plane Poiseuille flow with temperature dependent viscosity," *Int. J. Heat Mass Transfer* **36**, 2441 (1993).
- ¹¹M. Abramowitz and I. A. Stegun, *Handbook of Mathematical Functions* (Dover, New York, 1965).
- ¹²A. R. Wazzan, G. Keltner, T. T. Okamura, and A. M. O. Smith, "Spatial stability of stagnation water boundary layer with heat transfer," *Phys. Fluids* **15**, 2114 (1972).
- ¹³H. Herwig and P. Schäfer, "Influence of variable properties on the stability of two-dimensional boundary layers," *J. Fluid Mech.* **243**, 1 (1992).
- ¹⁴P. G. Drazin and W. H. Reid, *Hydrodynamic Stability* (Cambridge University Press, Cambridge, 1981).
- ¹⁵P. G. Simpkins and A. Liakopoulos, *Stability of Convective Flows* (American Society of Mechanical Engineers, New York, 1992).
- ¹⁶A. P. Hooper, "Long-wave instability at the interface between two viscous fluids: Thin layer effect," *Phys. Fluids* **28**, 1613 (1985).
- ¹⁷Y. Renardy, "Instability at the interface between two shearing fluids in a channel," *Phys. Fluids* **28**, 3441 (1985).
- ¹⁸D. D. Joseph, M. Renardy, and Y. Renardy, "Instability of the flow of two immiscible liquids with different viscosities in a pipe," *J. Fluid Mech.* **141**, 309 (1984).